Modeling and comparison of passive solar heating systems
by Robert Eugene Stotts

A thesis submitted in partial fulfillment of the requirements for the degree of MASTER OF SCIENCE in Mechanical Engineering
Montana State University

Abstract:
Computer models were developed to simulate and compare the thermal responses of direct gain, indirect gain, isolated gain, and natural passive solar heating systems. The performances of the direct and indirect gain models were verified using data from the passive test cells at the National Center for Appropriate Technology in Butte, Montana. A 139 m^2 (1500 ft2) home with standard insulation levels was used to compare the different types of passive solar heating systems. The collector area, thermal storage, and heating load were identical for the direct, indirect, and isolated gain systems. The natural passive system, which uses only the building and its contents for thermal storage and only south-facing windows for solar radiation collection, was simulated for several different collector areas. The largest collector area was approximately one half the area used in the other three systems. Comparisons of air temperature, auxiliary heating requirements, and solar fraction were performed for several different weather patterns, each of which had the same total insolation and the same ambient temperature variation. Each of the formal passive systems was found to supply more than half the heating needed by the home, with the direct gain system outperforming the Trombe wall (indirect gain) system for all of the weather patterns tested. The natural passive systems also provided significant solar heating, indicating that locating the normal window area present in a well insulated house on the south wall of the house results in a substantial solar fraction.

STATEMENT OF PERMISSION TO COPY

In presenting this thesis in partial fulfillment of the requirements for an advanced degree at Montana State University, I agree that the Library shall make it freely available for inspection. I further agree that permission for extensive copying of this thesis for scholarly purposes may be granted by my major professor, or, in his absence, by the Director of Libraries. It is understood that any copying or publication of this thesis for financial gain shall not be allowed without my written permission.

Signature Robert E. Stotts

Date Feb. 22, 1980

MODELING AND COMPARISON OF PASSIVE SOLAR HEATING SYSTEMS

by

ROBERT EUGENE STOTTS

A thesis submitted in partial fulfillment
of the requirements for the degree

of

MASTER OF SCIENCE

in

Mechanical Engineering

Approved:

Chairperson, Graduate Committee

Head, Major Department

Graduate Dean

MONTANA STATE UNIVERSITY
Bozeman, Montana

February, 1980

ACKNOWLEDGMENTS

The author wishes to thank Dr. R. O. Warrington and Dr. R. L. Mussulman for their help and guidance in the performance of this study. The author would also like to thank Dr. L. Palmiter of the National Center for Appropriate Technology for his valuable assistance in the validation of the computer models.

This study was supported by the Engineering Experiment Station at Montana State University, Bozeman, Montana.

TABLE OF CONTENTS

LIST OF TABLES

LIST OF FIGURES

NOMENCLATURE

Symbol	Description
a	distance from Z axis to window edge (see Figure 2.2)
A	Area
A_v'	vent area per unit width of storage wall (indirect gain)
b	distance from Y axis to window edge (see Figure 2.2)
b	storage wall thickness (indirect gain)
c	specific heat
c_p	specific heat at constant pressure (air)
C_a	Y-coordinate of arbitrary point Q (see Figure 2.1)
C_b	Z-coordinate of arbitrary point Q (see Figure 2.1)
C_d	vent discharge coefficient
DD	heating degree days, as defined by Equation (E.5)
DL	day length (hours)
DN	heating degree nights, as defined by Equation (E.7)
f(x)	initial storage wall temperature distribution
F_{A-B}	diffuse radiation view factor for radiation from surface A to surface B
g	acceleration due to gravity
Gr	Grashof number = $g\beta(T_w - T_\infty)x^3/\nu^2$
h	window height (see Figure 2.2)
h	heat transfer coefficient
$\bar{h}$	average heat transfer coefficient

Symbol	Description
h_0	heat transfer coefficient on window side of storage wall
h_b	heat transfer coefficient on interior side of storage wall
H	room height (see Figure 2.1)
H	storage wall height (indirect gain)
HS	daily total insolation
J	radiosity (total radiation which leaves a surface per unit time per unit area)
k	thermal conductivity of storage wall
l	window length (see Figure 2.2)
L	room length (see Figure 2.1)
m	mass
$\dot{m}$	mass flow rate of air
n	number of nodes in storage wall
$\overline{Nu}$	average Nusselt number = $\frac{\overline{h}L}{k}$
Pr	Prandtl number = $\frac{c_p \mu}{k}$
q_{ave}	average (numerical) solar flux, as defined by Equation (E.3)
q_s	solar flux, as defined by Equation (E.4)
Q_r	net total long-wavelength radiant heat transfer rate to a surface
Q_s	total absorbed insolation (rate)
r	infiltration rate (air changes per hour)
R	thermal resistance factor
SR	time of sunrise = $12 - \frac{DL}{2}$

Symbol	Description
SS	time of sunset = $12 + \frac{DL}{2}$
t	solar time (hours)
T	temperature (absolute)
T_{amb}	ambient temperature
T_{max}	daily maximum ambient temperature (see Figure E.2)
T_{mean}	average (numerical) ambient temperature, as defined by Equation (E.10)
T_{out}	vent outlet temperature (see Figure 2.6)
T_{space}	average air space temperature (see Figure 2.6)
T_w	storage wall temperature distribution
U	over-all heat transfer coefficient
UA_{tot}	heating load
W	room width (see Figure 2.1)
x	coordinate
y	coordinate
z	coordinate
α	surface azimuth angle of insolation (see Figure 2.1)
α	thermal diffusivity = $\frac{k}{\rho c}$
β	elevation angle of insolation (see Figure 2.1)
β	thermal expansion coefficient
γ	elevation angle of insolation, as projected onto X-Z plane (see Figure 2.2)
Δt	time step

Symbol	Description
Δx	node spacing (see Figure 2.7)
ε	long-wavelength radiation emittance
λ	dimensionless parameter, as defined by Equation (2.34)
μ	dynamic viscosity
ν	kinematic viscosity = $\frac{\mu}{\rho}$
ρ	density
σ	Stefan-Boltzmann constant = $5.669 \times 10^{-8} \frac{W}{m^2 \circ K^4}$

Subscripts

air	direct gain system air
i	surface (direct gain)
i	storage wall node
int	all interior surfaces except storage wall (lumped)
p	projection (in the insolation direction)
room	room air (indirect and isolated gain)
wall	storage wall
win	window
y	Y-coordinate

Superscripts

'	at the next time

ABSTRACT

Computer models were developed to simulate and compare the thermal responses of direct gain, indirect gain, isolated gain, and natural passive solar heating systems. The performances of the direct and indirect gain models were verified using data from the passive test cells at the National Center for Appropriate Technology in Butte, Montana. A 139 m^2 (1500 ft^2) home with standard insulation levels was used to compare the different types of passive solar heating systems. The collector area, thermal storage, and heating load were identical for the direct, indirect, and isolated gain systems. The natural passive system, which uses only the building and its contents for thermal storage and only south-facing windows for solar radiation collection, was simulated for several different collector areas. The largest collector area was approximately one half the area used in the other three systems. Comparisons of air temperature, auxiliary heating requirements, and solar fraction were performed for several different weather patterns, each of which had the same total insolation and the same ambient temperature variation. Each of the formal passive systems was found to supply more than half the heating needed by the home, with the direct gain system outperforming the Trombe wall (indirect gain) system for all of the weather patterns tested. The natural passive systems also provided significant solar heating, indicating that locating the normal window area present in a well insulated house on the south wall of the house results in a substantial solar fraction.

CHAPTER I

INTRODUCTION

Solar heating systems are receiving ever-increasing attention as alternate means of space heating. This is due to the spiraling costs of conventional (electric, gas, and oil) heating. Two basic types of solar heating systems, active and passive, are available. Active systems are characterized by collectors, pumps or fans, and elaborate heat delivery systems, such as plumbing or vents. They require a large initial capital investment and may require extensive maintenance. Control systems to regulate heat delivery to the building add to the complexity of these systems.

A passive solar heating system, on the other hand, is, by its very nature, an integral part of the building it heats. Passive systems consist of a large window (contained in the building's walls) for solar radiation collection and some means of thermal storage. The storage is usually a masonry material, such as bricks or concrete, or consists of water-filled containers. If the storage is distributed about the room containing the window, the system is referred to as a direct gain system. The thermal storage of indirect gain systems is concentrated into a wall a short distance from the window. This wall prevents most or all of the sunlight from entering the living space. Isolated gain systems are passive systems in which the collection and storage components are thermally isolated from the living space. A means of transferring heat from the storage to the living space, such as a fan, is necessary. One

example of this type of system is a solar greenhouse. Natural passive systems are direct gain systems with no added storage, other than the normal contents of the building. Thermal storage is only in the house itself and in its contents. Passive systems typically do not efficiently regulate heat delivery to their buildings. All the aforementioned passive systems, except the isolated gain types, rely on the thermal interactions between the various components of the system (window, storage and the building itself) to control the air temperature. During daylight hours, the large amounts of incident solar radiation (insolation) which pass through the window are mostly absorbed by the storage. This moderates peak daytime temperatures. At night, convection and radiation from the storage supply heat to the building. Since these interactions are functions of many variables (including the building heating characteristics, amount and type of storage, window area and type, and the ambient conditions), large air temperature fluctuations may occur. Indirect gain systems typically exhibit lower air temperature fluctuations than do direct gain or natural passive systems. Natural passive systems experience the largest fluctuations, due to their relatively small thermal storage. Isolated gain systems control the building air temperature much better than other types of systems, but high temperatures may occur within the collector.

Since passive systems are integral parts of the buildings they heat, they are not normally retrofitted. Instead, the storage and

window are incorporated into the building during original construction, often using the storage for structural support. In order to properly size the window area and storage for the system, some means of predicting its long-term performance, before it is built, is desirable. Rule-of-thumb methods are available to size the window area and the thermal storage [1]. However, these methods will not accurately (within 10%) predict the actual performance of the system. They are, however, useful for making a first guess.

Two other methods are also available for making an accurate prediction of the performance of passive systems. The first method is the use of computer models of the passive systems. The models are developed using basic thermodynamic and heat transfer equations to approximate the thermal response of the systems. F. Trombe [2] performed the first comprehensive modeling of the passive solar system commonly known as the Trombe wall system. It is an indirect gain system which uses a masonry wall, with vents at the top and bottom, for storage. Air flow from the living space through the vents transfers heat, by natural convection, to the living space. Extensive modeling of this system has been performed [3,4,5]. Several of these models were used to optimize various components of the Trombe wall system. Many of these models are also applicable to water wall systems. They are indirect gain systems which use water-filled containers for the storage wall. Models have also been developed to simulate the performance of direct gain systems [6,7]. The

first of these is a simple general model which is applicable to any type of passive system. The other is a model whose complexity rivals that of the direct gain model developed for this study. The model for this study was derived from basic principles. Little modeling has been done for natural passive and isolated gain systems.

When a passive solar system model is developed, some means of testing its performance is needed. This is usually done by using the model to simulate the experimentally measured performance of a system of the modeled type. Passive test cells are currently in use in several parts of the country to obtain the necessary data [8,9]. Some of this data was used to verify the performance of two of the models which were developed for this study. Models were developed to simulate the performance of direct, indirect (Trombe wall) and isolated gain systems. The direct gain model was also used to simulate the performance of natural passive solar systems.

The other method which is currently available to predict the performance of passive systems is a simplified method developed by Balcomb et al [10], at the Los Alamos Scientific Laboratories (LASL). The method is applicable to Trombe wall, water wall and direct gain systems. It estimates the performance of the systems as a function only of the building heating load, the monthly absorbed insolation and the total monthly heating degree days for the location of interest. Two additional climatic factors could be used to improve the method. The first

factor is the modification of degree days into degree days for daytime ambient temperatures and degree nights for nighttime ambient temperatures (see Appendix E). This modification has already been shown to increase the accuracy of simulations [11]. The second factor is a cloudy/clear day factor (CCDF). It would account for the differences in clear and cloudy day groupings for different geographical locations. The performance of all passive systems is dependent on the grouping of clear and cloudy days which occurs. The dependency on the CCDF is not yet known, but the simulations which were performed for this study represent the first step in determining this dependence. Simulations were performed for the various modeled systems (direct gain, indirect gain, isolated gain, and natural passive) for two different clear and cloudy day groupings. The natural passive system was simulated for two different window areas. The first approximated the normal window area present in a residence. The windows were assumed to all be on the south side of the building so that they could all provide solar heating. The second window area was approximately one half the window area present in the three formal passive systems. The window area, storage and heating load were identical for the three. The simulations formed a basis for a comparison of the performance of the four systems, for the two test cases. Comparisons of direct gain and Trombe wall systems have already been performed [12,13]. Direct gain systems without night window insulation were found to perform better (economically) than Trombe

wall systems with night window insulation in southern U.S. climates. However, Trombe wall systems with night insulation were found to be more economical that direct gain systems with night insulation in northern U.S. climates. None of these studies includes isolated gain or natural passive systems. Since data for verification of these two models were not available, the results of their simulations are only preliminary and should be treated accordingly.

CHAPTER II

ANALYTICAL MODELS

The differential equations which were used to develop the passive solar system models were obtained from basic principles. Basic thermodynamic laws were combined with theoretical and empirical heat transfer equations. A few simplifying assumptions were used to reduce the complexity of the problems.

Direct Gain Model

This model was developed for a single room with a single window. It could, however, be easily expanded to model a more complex building, such as an entire dwelling. To obtain high accuracy and generality, all modes of heat transfer within the room were assumed to be important. Radiative exchange among the walls, floor, ceiling, and window was incorporated into the model. Convection from each surface in the room to the room air and conduction from these surfaces, through the walls, to the ambient were also computed. The desired degree of accuracy necessitated knowing the size, location and shape of the sunlit areas within the room. This resulted in a complex geometry problem.

Figure 2.1 illustrates the geometry of the modeled direct gain system. Sunlight enters the room through the window at an elevation angle β and a surface azimuth angle α. Morning sun has a positive α. The entering sunlight may fall, in part or in full, on the floor or on any of the north, west, and east walls. For this model, the sunlit portion

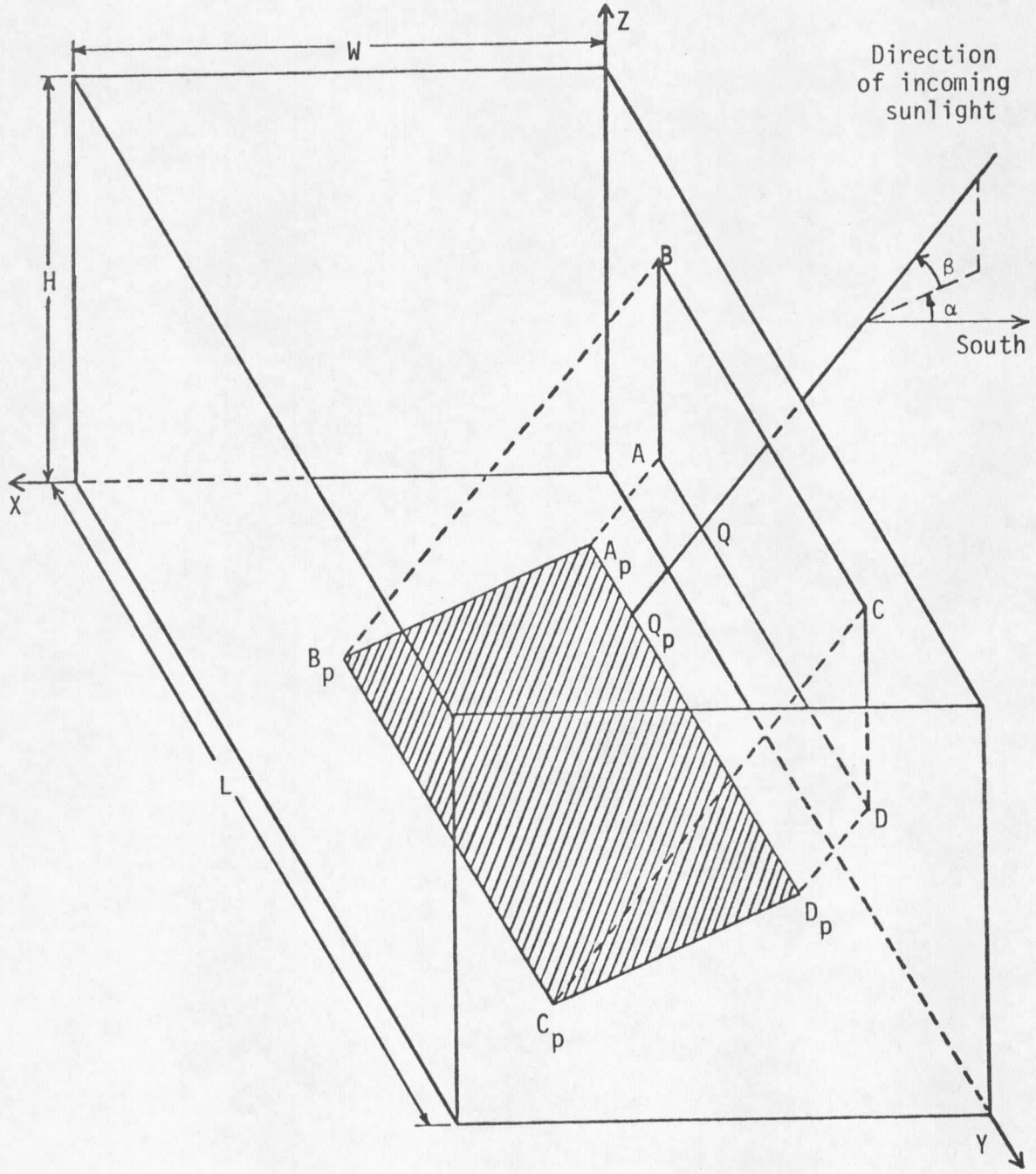

Figure 2.1 Configuration and Nomenclature of the Direct Gain System

of each of these surfaces was treated as an individual surface.

During the course of a normal day, the size, location and shape of the sunlit areas within the room change continuously. These are functions only of the room geometry and the direction of the incident solar radiation (insolation). The direction of the insolation (α and β) was calculated using relations from Duffie and Beckman [14]. These angles are functions only of the window orientation (azimuth angle and slope), the latitude, the time of day and the day of the year. Provision was made in the model for a non-vertical, non-south-facing window.

Once the insolation direction was known, the size, location and shape of the sunlit areas were found. The first step in this was to locate the projections (in the direction of the insolation) of the corner points of the window. For example, consider any point Q on the south wall of the room, as shown in Figure 2.1. The coordinates of point Q are $(0,C_a,C_b)$. Expressions for the coordinates of its projection, Q_p, are given in Table 2.1, as a function of where the projected point falls. In these equations, the angle γ (see Figure 2.2) is defined as

$$\gamma = \tan^{-1}(\tan \beta/\cos \alpha). \qquad (2.1)$$

Obviously, with four different sets of equations for the coordinates of Q_p, some means of determining which surface the point intersected was needed. One method of accomplishing this determination would be to

Table 2.1 Equations for the Coordinates of Point Q_p

Coordinate	Q_p falls on the floor	north wall	west wall	east wall	Limits
X	$C_b \cot\gamma$	W	$(L - C_a)\cot\alpha$	$-C_a\cot\alpha$	$0 \leq X \leq W$
Y	$C_a + C_b \tan\alpha \cot\gamma$	$C_a + W\tan\alpha$	L	0	$0 \leq Y \leq L$
Z	0	$C_b - W\tan\gamma$	$C_b - (L-C_a)\tan\gamma\cot\alpha$	$C_b + C_a \tan\gamma \cot\alpha$	$0 \leq Z \leq C_b$

Table 2.2 Coordinates of the Window Corner Points

Corner Point	Coordinates
A	(0,a,b)
B	(0,a,b+h)
C	(0,a+l,b+h)
D	(0,a+l,b)

calculate the coordinates of the projected point with each of the sets of equations and compare the results of each set with the allowable limits of each coordinate. The limits are listed in Table 2.1. The selection criteria were based on this method, but were condensed into a smaller set of inequalities which, when satisfied, determined the location of the projected point. These selection criteria are given in Appendix A. The projections of the window corner points were found using this method. The coordinates of the corner points (to be used in the equations in Table 2.1) are given in Table 2.2.

After locating A_p, B_p, C_p, and D_p, the size, shape and location of the sunlit areas were calculated. There were 19 possible configurations for the sunlit areas. These possibilities were designated by the set of locations of the projected window corner points. For example, one such set is {A_p, B_p, and D_p on the floor and C_p on the west wall}. This configuration is illustrated in Figure 2.2. The shaded areas represent the sunlit portions of the room. Appendix B contains a list of all the possible configurations that the sunlit areas may assume. Also included is a brief description of the method which was used to determine which configuration occurred for any insolation direction.

It is apparent from Figure 2.2 that the sunlit areas in the room have complex geometrical shapes which change continuously throughout the day. For this reason, and since diffuse radiation view factors are difficult to calculate for odd shapes, an equivalent rectangle was